

EVOLUTION & DEVELOPMENT OF VISUAL ODEMETRY SYSTEMS

REDDY B.L.

Department of CSE, KL UNIVERSITY,
Vaddeswaram, India

ABSTRACT

With speedy improvements inside the place of cellular robotics and industrial automation, a growing need has arisen in the direction of accurate navigation and localization of shifting items. camera based motion estimation is one such approach that is gaining big recognition as a result of its simplicity and use of confined assets in generating movement route. while a wheeled robot operates in a slippery surroundings, visual Odometry, which is used to gain flow-snap shots of the floor with a CCD camera, is effective for the size of movement due to the fact it's miles a non-touch method .however, inside the target condition, a dimension result with a conventional digicam isn't always dependable with this technique because the viewing place of the floor varies because of the changing distance among the camera and the floor because of the wheels sinking in free soil .To clear up this hassle, we used a telecentric digital camera for visible odometry whose lens maintains the equal discipline of view with a change of distance among the digital camera and the ground. the use of the camera, we evolved a three-dimensional odometry device for our mobile robot to permit its positioning and navigation, and we proven the gadget with numerous experiments. in this paper, a structure and a performance test of the evolved system is defined. After that, the results of experiments in indoor (sandbox) and outside (seashore) environments are introduced.

KEYWORDS: mobile robot positioning, visual odometry, telecentric camera, motion estimation ,VO datasets.

INTRODUCTION: With growing automation in specific engineering fields, cell robotics is gaining massive reputation. The unmanned car is one such proliferating instance this is increasing its fleet in specific applications ranging from business to strategic use. one of the

simplest mechanism to estimate the movement of a terrestrial car is to apply wheel encoders. but, these have limited utilization in ground automobiles and be afflicted by inaccuracies that occur due to wheel slippage at some stage in motion in muddy, slippery, sandy or free terrains. The errors bobbing up at every immediate receives amassed over time and the predicted pose drifts in share to the space traveled. conventional navigation processes together with inertial navigation structures (INS), the worldwide positioning machine (GPS), SONAR, RADAR, and LIDAR are presently in use for exceptional packages. Unavailability of GPS signals in an indoor and under-surface surroundings, unacceptable excessive glide the usage of inertial sensors throughout prolonged GPS outages, troubles of feasible confusion with close by robots for SONAR & RADAR, and the line of sight requirement for laser-based structures are a number of the constraints related to these navigation structures. one of the promising answers lies inside the art of visible odometry that helps in estimating movement information with the assist of cameras hooked up over the vehicle.

The onboard vision device tracks visible landmarks to estimate rotation and translation among two-time instants. The art of imaginative and prescient-based navigation is stimulated by means of the conduct of a fowl which relies closely on its imaginative and prescient for guidance

and manage [3]. The initial works on estimating motion from a digicam by has helped in setting up the visible odometry (VO) pipeline. Simultaneous localization and mapping (SLAM), a superset of VO, localizes and builds a map of its surroundings together with the trajectory of a shifting object. however, the discussion in this paper is constrained to visual odometry, which incrementally estimates the camera pose and refines it using optimization approach. a visual odometry device includes a specific camera association, the software program architecture and the hardware platform to yield camera pose at every time immediate. The digital camera pose estimation can be both look or function based. the arrival-based strategies operate on depth values at once and fits template of sub-pics over frame or the optical waft values to estimate motion. The function-primarily based strategies extract wonderful hobby points that may be tracked with the help of vectors describing the nearby region around the key-factors. these strategies are depending on the image texture and are generally no longer applicable in texture-much less or low texture environments such as sandy soil, asphalt, and so forth. The VO technique can also be labeled as geometric and gaining knowledge of based. The geometric VO strategies are those that explore camera geometry for estimating movement while the studying based VO scheme trains regression model to estimate movement parameter while fed with classified facts. The studying-primarily based VO approach does not require the camera parameters to be recognized initially and can estimate trajectories with correct scale even for monocular cases .

Applications : The VO scheme may be implemented either with a monocular, stereo, or RGB-D digital camera relying at the system design. Stereo VO mimics the human imaginative and prescient machine and may estimate the photo scale right now in contrast to monocular VO. however, stereo camera systems require extra calibration attempt and stringent digital camera synchronization with out which the mistake propagates through the years. The monocular digicam is desired for cheaper and small form element programs such as cellphone, pc, and many others. in which the mounting of cameras with a certain baseline is not constantly viable. some of the tactics that aimed to get better scale records for monocular VO are the usage of IMU facts, optimization method all through loop closure , and incorporating recognized dimensional statistics from walls, buildings, and so on. An RGB-D camera presents color and depth facts for each pixel in an image. The RGB-DVO starts offevolved with the 3-d position of characteristic factors that are then used to acquire transformation thru iterative closest factor algorithm. The VO scheme has discovered its principal application inside the car industry in motive force assistance and self sufficient navigation. one of the packages of visible odometry has been to estimate car movement from the rear-parking digicam and use this statistics with GPS to offer accurate localization . The assignment of visible serving (moving the camera to a preferred orientation) could be very similar to the visible odometry hassle requiring pose estimation for a special cause. these schemes are not best useful for navigation of rovers on surfaces of different planets including Mars however also are useful for

monitoring of satellites that needs to be repaired the use of a servicer.

Goals : increase a running prototype of digicam movement estimation based on the pics captured with the aid of the digital camera. very last path of digital camera movement is obtained by way of concatenating the man or woman poses. The challenge ambitions to develop the machine for the ground car and UAV programs.

Limitations :

Even though these VO strategies have proven promising outcomes for variety of those applications, they're touchy to environmental changes such as lighting fixtures situations, surrounding texture, the presence of water, snow, and many others. a number of the alternative situations that cause poor monitoring records are motion blur, the presence of shadows, visual similarity, degenerate configuration, and occlusions. at the side of these, some man-made errors also creep into the facts at some point of image acquisition and processing steps including lens distortion and calibration, feature matching, triangulation, trajectory drift due to lifeless-reckoning which result in outliers. therefore, the VO schemes need to be robust and have the capacity to manipulate those issues correctly.

METHODOLOGY :

A. Geometric Approaches: Feature-based

The research on visual odometry observed it's origin lower back in 1960's where a lunar rover was constructed by means of Stanford university for controlling it from

the Earth. This cart changed into in addition explored by way of Moravec to demonstrate correspondence based totally stereo navigation technique in 1980. This scheme matches wonderful function between stereo snap shots and triangulates them to the 3-D international body. as soon as the robot movements, those characteristic points are matched in the subsequent frame to gain corresponding 3-D factor and generate movement parameters. Mattheis and Shafer advanced upon this technique via modeling the triangulation mistakes as 3-D Gaussian distribution in place of scalar weights. Arun et al. proposed a least square based totally approach for figuring out a metamorphosis between 3-D point clouds. Weng et al. proposed a matrix-weighted least rectangular answer which performed remarkably higher than unweighted or scalar-weighted solution. It also proposes an iterative top of the line scheme to gain motion parameters and three-D factors. some of the researchers employed Kalman filtering to estimate movement parameters by means of modeling the noise in photo records with the aid of Gaussian distribution. Olson et al. solves the movement estimation trouble thru a most-likelihood system and mentions the use of an absolute orientation sensor to reduce the mistake growth price for long distance navigation.

exceptional formulations to solve function-primarily based VO have been discussed within the literature earlier than 2000 and is also gift in the literature in assessment articles. therefore, not lots of it will likely be discussed right here and the main emphasis might be to provide the upgrades in function-based VO schemes chronologically publish 2000 generation. In 2002, Se et al. proposed to apply scale

invariant characteristic, SIFT for monitoring hobby points throughout photo frames and estimation ego-motion wrong photo calibration, function mismatch, picture noise, and triangulation errors are some of the contributing factor in the direction of outliers at some point of pose estimation. numerous outlier rejection schemes for strong estimation which include RANSAC, MLESAC and their versions have been proposed in the literature. a number of the researchers geared toward estimating movement parameters while not having a priori information of digicam calibration parameters. but, knowing the intrinsic parameters in advance facilitates in obtaining greater correct and sturdy movement estimate mainly for planar or near planar scenes. The step-by way of-step motion estimation framework for each the monocular & stereo instances and coined the popular time period 'visible odometry' in this Paper. Later, Engels et al. estimated pose using this 5-factor algorithm observed with the aid of a package deal adjustment based refinement method. Se et al. applied Hough remodel and RANSAC approach for obtaining a consistent set of fits over which the least rectangular minimization is implemented to gain pose estimation. It has additionally contributed towards using smaller characteristic descriptor of length 16 with enough discriminative strength to healthy capabilities, motivating researchers for more efficient feature descriptors. Tardif et al. predicted rotation using epipolar geometry and translation the use of 3D map while optimizing the current place by myself, as opposed to all previous places as finished in bundle adjustment. good sized work has additionally been pronounced closer to simultaneous

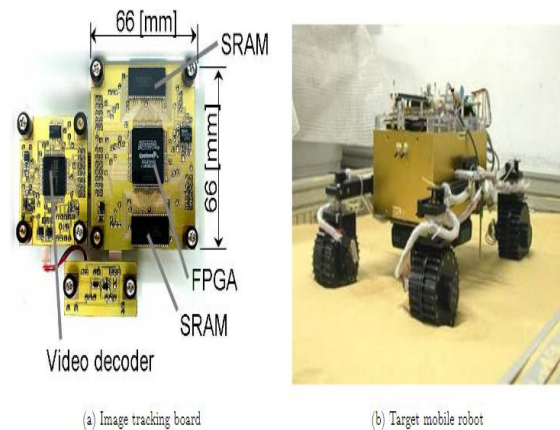
localization and mapping (a superset of pose estimation) all through this time and later, however is not discussed on this paper.

until this time, good sized work were said on exceptional motion estimation sub-exercises which includes estimating movement from exclusive camera types, estimating calibration & critical matrix, and pose refinement the use of package deal adjustment which contributed closer to accuracy improvement. With this growing self belief on function-primarily based VO techniques and its demonstration on floor automobile navigation, it become utilized in navigating Mars exploration rover. It then received renewed hobby some of the researchers and numerous improvements had been proposed within the literature. Kaess et al. used glide information for segregating remote and close factors and predicted rotation and translation from them separately. Proposed a pose estimation set of rules the use of three points and the expertise of vertical course acquired from IMU or the vanishing factor. however, this scheme turned into not able to provide closed-form solution and had singularity troubles. Naroditsky et al. offered a closed shape solution the use of comparable 3-plus-one set of rules by the usage of vanishing point or gravitational vector as the reference. Later, in 2011 Scaramuzza et al. proposed the 1-point algorithm for motion estimation with the aid of utilizing the non-holonomic constraints of wheeled motors which switches to the same old 5-factor algorithm on detection of lesser inliers. Lee et al. extended this paintings for multi-camera set-up by modelling it as a generalized digicam and proposed a 2-factor algorithm for obtaining the

dimensions metric. song et al. proposed a multi-thread monocular visible odometry approach that doesn't require any assumption concerning the environment for scale estimation. Epipolar seek in most of these threads with insertion of continual 3D points at key-frames helped in improving its accuracy and pace. Persson et al. prolonged this approach via generalizing it for the stereo case. The three-D correspondences and the pose predicted through movement model is used to predict music function and in refinement process.

Badino et al. improves the positional accuracy of characteristic points through averaging its role over all its preceding occurrences and use these integrated features for improving ego-motion accuracy paid importance to the camera calibration parameters and corrects them with the aid of matching function factors from one body to the other with to be had floor fact movement. Cvisic & Petrovic used a aggregate of stereo and monocular VO for estimating rotation the usage of five-factor algorithm and translation through minimizing re-projection error as achieved for the stereo case. Rotation estimating via monocular case help in overcoming mistakes springing up due to imperfect calibration at the same time as translation estimation thru stereo case increases the accuracy. Bellavia et al. proposed a key-body selection approach primarily based on the existence of photograph factors with sufficient displacement. Liu et al. proposed an improvement over the RANSAC scheme by using producing the hypothesis preferentially and the usage of three nice hypotheses to estimate motion.

1. Conventional visual odometry system :



To determine the diploma to which the trade inside the picture scale affects the accuracy of the odometry, we installed a visual odometry gadget at the cellular robotic. figure (a) is a picture of the visible tracking board. it's far a device used to estimate the translational pace through monitoring the glide of ground capabilities with an NTSC camera. The tool is composed often of a video decoder, which converts the analog picture sign from the NTSC to a digital photo, SRAM, which stores photos, and FPGA, which performs image monitoring. it could degree as much as a speed of 96 [pixel/frame] in an arbitrary aircraft at the frame charge. The measured facts is transferred through a serial connection. For an NTSC digital camera, we used a regular CCD camera (Watec WAT-902B), which has a horizontal attitude of view of 24.2[deg]. The above visible odometry machine changed into hooked up on the cellular robot proven in the determine(b).

2. Algorithm of ground-pattern tracking :

To song the ground-sample for visual odometry, Nagai proposed a tracking algorithm that is robust in a natural

colorless pattern. The algorithm changed into validated on grass, carpet, and a strawtatamimat .discern 3 shows an photograph of Toyoura sand.A characteristic of the set of rules is to use a set of reference factors in preference to template blocks. The reference factors have discrete location and solidly move in line with photograph monitoring. The motion ofthe photo functions between the 2 frames is acquired with the aid of calculating the interface correlation of the group of reference points. It isn't always appropriate to extract and music a few gadgets in a video picture, however itis powerful to tune the total picture glide. similarly, it's miles suitable for FPGA-based logic to implement on a small board, as shown in determine 2-(a). In our implementation, the wide variety of reference points is256; maximum speed is from -31 to ninety six [pixel/frame] (x-path) and from -31 to 32 [pixel/frame](y-path). information of the set of rules and implementation are defined in the underneath discern.

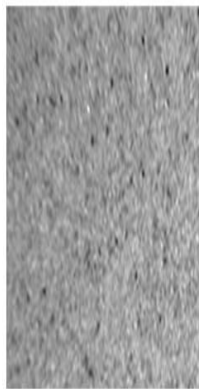


Figure 3: Image of Toyoura sand from the telecentric camera

3 Initial comparison experiment :

We set up the above visual odometry gadget on our mobile robotic and conducted two simple experiments. The conditions had been as follows.

- Circumferential velocity of the wheel : 3 [cm/sec]•traveling distance : eighty [cm]•floor : P-tile and smooth soil (Toyouura-sand)In gentle soil, whilst the robotic started out moving, each wheel started out sinking till it have become solid. eventually, the subsidence of the wheel become 35[mm]. discern 4 indicates the envisioned paths and the actual course, which is called “ground reality” .The floor fact became measured by an optical instrument called “general station” produced by Nikon Trimble. it is a combination of an electronic theodolite (transit) and an electronic distance meter to detect the gap to a target corner cube. It additionally has an automated monitoring system of the goal; therefore it obtains a transition record of the goal. The target corner cube is set up on the middle pinnacle of the robotic. according to the Nikon Trimble catalog, the accuracy of the size of moving items is less than 1[cm].

down, and a the distance among the digicam and the ground changes. at some point of this manner, the hueof the ground picture zooms in and out, which prevents accurate matching for visible monitoring. discern 5shows the transition of a robotic's velocity measured by using our visible odometry. within the first 4 seconds of the parent, the velocity of the robotic measured with the visible odometry device is risky. We expect that the matching system failed due to the changes inside the hue of the ground photos .the two issues described above motivated us to expand a new visible odometry gadget, which isdescribed within the following sections.

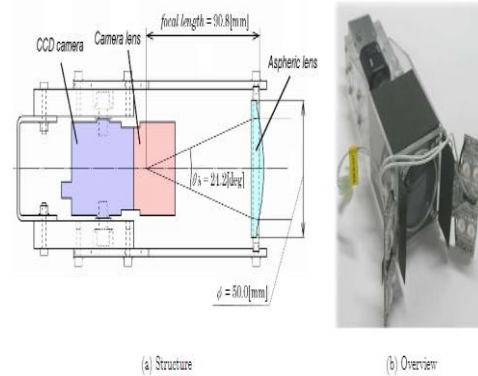
3. DEVELOPMENT OF A TELECENTRIC MOTION MEASUREMENT SYSTEM

It was very hard to obtain a huge vicinity telecentric lens commercially, therefore, we developed our own object-aspect telecentric optical gadget. The parameters of our telecentric optics are described below. Our objective changed into to estimate the placement of a small mobile robot on unfastened soil. Its maximum velocity become set as one hundred [mm/sec]. using a general CCD digital camera with a frame charge of 30 frames per second, a machine is needed to measure three.33 [mm/frame]. Our visual monitoring board has the capability to measure ninety six [pixel/frame], and the effective pixels of the longitudinal/horizontal axis of the photograph is 512 [pixels]. consequently, the gap from the middle to the threshold of the viewing vicinity ($W/2$) is calculated as follows

$$W/2 = (3.33 * 512) / 96 = 17.8 \text{ [mm]} \quad (1)$$

which means the minimal diameter W of the lens need to be large than 17.78×2 . To maintain on the safe aspect, we selected a industrial aspheric surface convex lens (aperture = 50 [mm], focal duration = ninety.eight [mm]), synthetic via Ikuta Seimitsu Co., Ltd. when the lens is placed 90.8 [mm] away from the origin of the sector attitude of the camera lens, it configures the telecentric optical gadget. If the focal length is shorter, smaller telecentric optics can be configured. however, in this situation, the digital camera-side lens should be a huge-angle

lens that generates a huge deformation. The focal period turned into decided by trial and blunders.

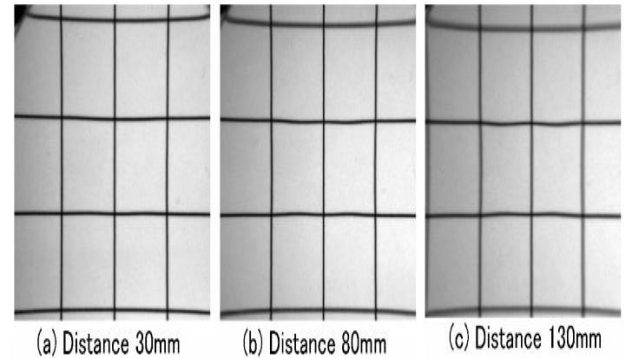
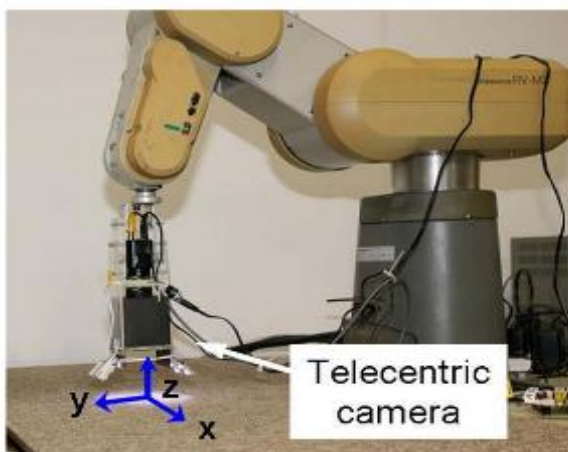


On the other hand, the camera lens is required to have a field angle as $\tan^{-1}(17.78/90.8) \times 2 = 22.16 \text{ [deg]}$

, therefore we chose EMVL-MP1214 (focal length = 12.0 [mm], horizontal field angle = 24.2 [deg]) made by Misumi Group Inc. as a standard c-mount camera-side lens. Due to the above parameters, the distance per pixel (resolution) is calculated as 0.0723 [mm]. According to our initial experiment, it has a constant field of view regardless of the distance between the lens and the target from 3.0 [cm] to 13.0 [cm]. Figure 6-(a) shows a schematic of the developed tele-centric camera that includes the CCD camera and lens layout, and Figure 6-(b) shows our hand-made telecentric camera. Finally, our conventional camera shown in the previous section was replaced from the telecentric camera to conform a telecentric motion measurement system. We also mounted 8 white LEDs at the side of the aspheric lens to gain a lightness contrast of an image.

Initial performance tests:

to assess the measurement accuracy of the evolved movement dimension system, which contains the above-described telecentric optics, simple experiments had been carried out. We connected the telecentric camera to the top of a manipulator arm. The motions of the camera had been generated by using controlling the arm, which led to very accurate position management of the digital camera. Figure 7 is a top level view of the experimental setup. Figure 8 indicates three photographs of the grid sheet acquired through the telecentric digital camera with different distances from the floor. The cost of the gap (z-axis) was changed to 30 [mm], eighty [mm], and 130 [mm]. Each grid size is 10 [mm] squares. The photograph scales do not alternate with diverse distances from the digital camera. that is the maximum vital function for the telecentric motion size machine. The digital camera changed into then moved in a brief distance over a traditional carpet pattern the usage of the manipulator arm at a mean pace of 15 [mm/s]. performance assessments for the translational motion of the telecentric camera were conducted in the following three patterns:



Pattern 1: Moving the camera from (-50, 0, 30) to (50, 0, 30)

Pattern 2: Moving the camera from (-50, 0, 130) to (50, 0, 130)

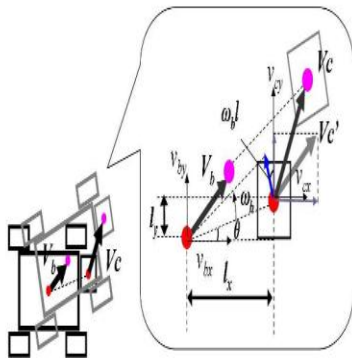
Pattern 3: Moving the camera from (-50, 0, 30) to (50, 0, 130)

where the coordinate axes are shown in Figure 7. The motion patterns were repeated 20 times, and the maximum error of length and maximum standard deviation were calculated. Table 1 shows the results of the experiment. The results indicate that the maximum measurement error was 2.36 % and the maximum standard deviation was 0.47 %. We conclude that the errors of translation of the proposed system are small enough for the measurement of a mobile robot's transition.

Implementation of visual odometry for mobile robots:

In order to apply the telecentric motion measurement system to a visual odometry for our mobile robot, two issues have to be resolved. The first is how to compensate for an instruction offset of the camera to

Pattern / Orientation	Error %	Std. deviation %
Pattern 1 / x-axis	2.26	0.16
Pattern 1 / y-axis	1.26	0.34
Pattern 2 / x-axis	0.46	0.07
Pattern 2 / y-axis	2.10	0.47
Pattern 3 / x-axis	0.66	0.07
Pattern 3 / y-axis	2.36	0.40



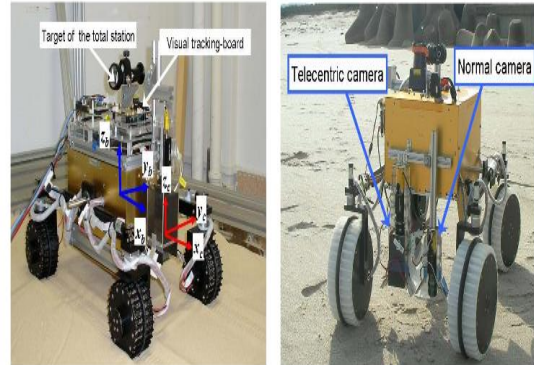
gain translational pace, and the second is the way to realize three-dimensional odometry. A superficial translation velocity for the sensor is generated through a summation of a translational velocity and a rotational speed of the robot frame. therefore the superficial translation pace is compensated for via a measurement of the rotational velocity (Fig. 9). To measure the rotational velocity, we used a gyroscope to discover the yaw attitude on the robot. The translational velocity of the robotic body (v_x, v_y) changed into then calculated the use of the subsequent equation:

$$\begin{cases} v_{x'} = v_x + l\omega_y \sin\theta \\ v_{y'} = v_y - l\omega_x \cos\theta \end{cases} \quad (2)$$

$$l = \sqrt{l_x^2 + l_y^2} \quad (3)$$

$$\theta = \tan^{-1}\left(\frac{l_y}{l_x}\right) \quad (4)$$

where, v_x and v_y are the velocities in the X direction and the Y direction, respectively, obtained by the telecentric motion measurement system, ω is the angular velocity of the robot body, and l_x and l_y are, respectively, the offset lengths of the camera in the robot coordinate system. For our robot, l_x is set as 200 [mm], and l_y is set as 0 [mm].



(a) Rover test bed A

(b) Rover test bed B

For the latter problem, we use three gyroscopes for the dimension of the roll, pitch, and yaw angles of the robotic body. Then, v_x and v_y , obtained via the Equation (2)-(four), are translated into an inertial coordinate machine using the Euler angle conversion. by means of calculating the integration of the velocities in the inertial coordinate system, the robotic's function and attitude are calculated three-dimensionally. The above implementation changed into done on our cellular robot testbed, and several assessment experiments have been carried out. they are shown inside the following segment.

EXPERIMENTS:

To confirm the validity and the limitation of our developed system, we performed the following three experiments.

Experiment 1 : Checked robustness against change of distance between camera and the ground.

Experiment 2 : Checked maximum velocity of the measurement.

Experiment 3 : Performed outside tests

Experimental setup :

We used each small and center-length rover testbeds, as proven in figure 10. both rovers have the same structure. they're four-wheeled robots that had been developed by means of our research group. every of the wheel has two cars, one for riding and one for guidance, and each may be managed independently. The wheels are connected to the main body via a rocker suspension. The testbed (a) is 55 centimeters in length, 38 centimeters in width, 30 centimeters in top, and weights approximately thirteen kilograms. The testbed (b) is 81 centimeters in length, 51 centimeters in width, forty three centimeters in top, and weights about 24 kilograms. In each testbeds (a) and (b), a telecentric camera and a everyday digital camera have been set up in the front/rear middle of the robot. the gap between the everyday digicam and the ground was set to keep the identical photo as that of the telecentric camera whilst the wheels have been on a hard floor. To degree a robot's floor fact, we use the total station added in section 2.three. We used testbed (a) for Experiments 1 and 2 and testbed (b) for experiment 3

Experiment 1: Checking robustness against the change of distance between the camera and the ground

inside the first test, we ran the rover testbed (a) for 80 [cm] on an eight[deg] tilted sandbox that contained Toyoura sand (very quality-grained sand). We carried out this experiment in 3 times. Figures eleven-

(a) and (b) display one of the comparisons of the dimension outcomes between a telecentric digicam and a ordinary digicam. The dimension effects the use of a telecentric digital camera (red line) suit the floor reality (black line), but a big degree of error was noted while the regular digital camera turned into used. in the 3 experiments, the common mistakes with the telecentric camera changed into 2.7 % (fashionable deviation is zero.38 %), and the common blunders with the ordinary digital camera was 53.1 % (general deviation is 5.15 %). For reference, the common length of measurement results with the traditional wheeled odometry was 800 [cm], ten times large than the ground reality. In both cases, when the robot commenced moving, every wheel commenced sinking (Fig.12-(a)) until it have become strong (Fig.12-(b)). the space among the digicam and the ground then changed from the initial condition to the final situation. visual sinkage of the wheel turned into approximately three.0[cm]. which means that the gap between the camera and the ground changed from 8[cm] to five[cm], which suggests that the appearance of gadgets in its image is magnified 1.6 times. therefore, the order of the error price is reasonable, and the telecentric digicam works properly in such situations.

Experiment 2: Checking the maximum speed of the measurement

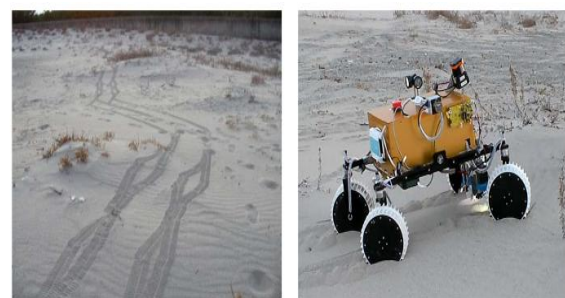
Theoretically, the maximum size speed of the telecentric motion measurement machine is 96[pixel/frame], that is identical to 208 [mm/sec]. To confirm the value, we carried out one simple experiment to verify the most measurement velocity. on the flat sand-box packed with

Toyoura sand, we modified the reference speed of the wheels. We also recorded the measurement pace by the telecentric movement measurement machine and its actual velocity by means of the overall station, introduced in phase 2.3. sooner or later, we in comparison the both profiles of velocities. The effects of the above experiment indicated that the telecentric motion size system measured step by step as much as 100 [mm/sec], and it could not measure over 110 [mm/sec]. It did not reach the theoretical fee. We assumed that the primary reason became a lighting situation: it became now not sufficient to cover whole place by way of 8 white LEDs. the idea turned into showed via another test in which the device measured around 140 [mm/sec] in case of current an external light on a carpet floor. In our current configuration, it satisfied the conventional planetary rover velocity. consequently we did not add additional LEDs.

Experiment 3: Performance test in long-distance navigation

We performed outdoor experiments the usage of a middle-sized rover testbed (Fig.10-(b)) on the seashore in Miyagi Prefecture, Japan (Fig.thirteen-(a)). within the experiments, we set the rover's speed as 40 [mm/sec]. We executed several take a look at runs in numerous situations, and the whole navigation length of the experiment was approximately a hundred [m]. one of the size consequences is proven in parent 14. In this example, the navigation length changed into approximately 20 meters, and the first 6 meters changed into a mild up-slope. in line with the graph, the measurement end result via the visible odometry with a

ordinary digital camera includes a big degree of blunders. On the other hand, the measurement end result with the aid of the telecentric movement dimension system corresponds with the ground truth. mistakes comparison on the very last role, obtained via the wheeled odometry, the visual odometry with a ordinary digicam, and the telecentric motion size device, is proven in table 2. The result indicates a validity of the proposed system in outdoor environments.



(a) Overview of the experimental field

(b) Rover navigating on a slope

DISCUSSIONS :

In determine 4-(a), it's far apparent that visual odometry returns a completely correct function of the robot and is independent from wheel slippage. however, because of wheel sinkage, we showed the following two major issues. One problem is the distinction in scale. If the gap between the camera and the floor is fixed, the performance of the visible odometry is superb, which is showed in figure 4-(a). but, because of adjustments inside the distance between the camera and the floor, the accuracy of a robotic's position decreases, proven in parent 4-(b). If the digital camera is installed high sufficient, the impact of the sinkage of the wheel at the digicam scale is fantastically small. however, such situations are tough for small robots. furthermore, the floor pattern might not be detected with a the high-hooked up digicam. the other hassle is

the failure of monitoring, when the soil parameter modifications, the wheels pass up or down, and a the distance among the digicam and the ground adjustments. at some stage in this system, the hueof the ground image zooms in and out, which prevents correct matching for visible tracking. determine 5shows the transition of a robotic's velocity measured by way of our visible odometry. inside the first 4 seconds of thefigure, the speed of the robot measured with the visible odometry gadget is unstable. We expect thatthe matching procedure failed due to the changes in the hue of the ground images.the 2 problems described above prompted us to increase a brand new visual odometry machine, which isdescribed within the following sections.

animplementation of the 3 dimensional visual odometry the use of the advanced device. The experimentalresults varidated the robustness with the sinkage of the wheels. mainly, in step with the finalexperiment, which evaluated long-distance navigation, the usefulness of the machine turned into confirmed in areal environment.these days, in our studies group, the telecentric movement dimension device has been used not onlyto degree the robotic's position and orientation but also to achieve the slip ratios of the robot's wheelson free soil, which may be very essential for the analysis of the interaction between the wheel and the soil. Now, it seems to be a dependable and considered necessary device for research on planetary rovers. but,based totally on our modern implementation, it seems tough to apply this kind of system to quicker robots. This, ofcourse, relies upon on the computational power, ground patterns, and diameter length of the aspheric lens.In destiny works, we would love to expand a smaller gadget and a quicker size pace.

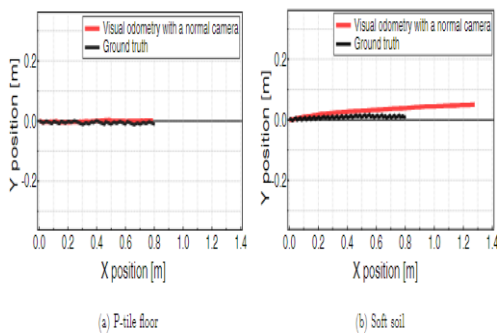
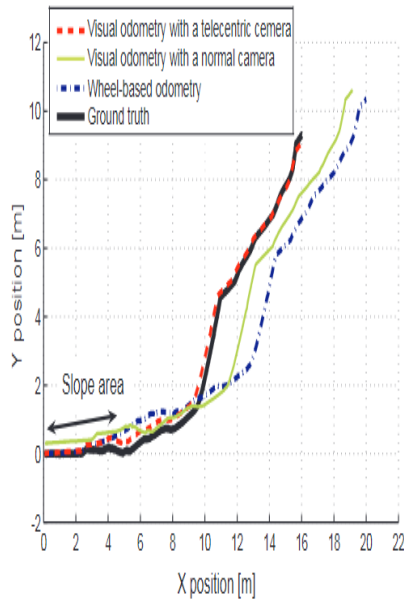


Figure 4: Comparison of experimental trajectories on sand for straight travel

CONCLUSIONS AND FURTHER DEVELOPMENTS :

on this paper, we delivered the development of a telecentric motion dimension gadget for thepositioning of wheeled mobile robots on unfastened soil, along with that on Mars or the moon. A key characteristic ofthe system is the usage of the telecentric optics evolved in this studies. The preliminary experimental resultconfirmed that the dimension error of the evolved machine become much less than three % We then introduced

Odometry method	Error in x-axis %	Error in y-axis %
Wheeled odometry	24.8	11.3
Visual odometry with a normal camera	18.8	10.7
Telecentric motion measurement system	0.1	2.4



REFERENCES :

[1] Phillip John McKerrow. *Introduction to Robotics*. Addison Wesley, 1991.

[2] Genya Ishigami, Akiko Miwa, Keiji Nagatani, and Kazuya Yoshida. *Terramechanics-based model for steering maneuver of planetary exploration rovers on loose soil*. *Journal of Field Robotics*, 24(3):233–250, 2007.

[3] J. Y. Wong. *Theory of Ground Vehicles*. John Wiley & Sons, 1978.

[4] Hans Moravec and D.B. Gennery. *Cart project progress report*. July 1976.

[5] Daniel M. Helmick, Stergios I. Roumeliotis, Yang Cheng, Daniel S. Clouse, Max Bajracharya, and Larry H. Matthies. *Slip-compensated path following for planetary exploration rovers*. *Advanced Robotics*, 20(11):1257–1280, 2006.

[6] Mark Maimone, Yang Cheng, and Larry Matthies. *Two years of visual odometry on the mars exploration rovers: Field reports*. *Journal of Field Robotics*, 24(3):169–186, 2007.

[7] S.S. Beauchemin and J.L. Barron. *The computation of optical flow*. *ACM Computing Surveys (CSUR)*, 27(3):433–466, 1995.

[8] David Nister, Oleg Naroditsky, and James Bergen. *Visual odometry for ground vehicle applications*. *Journal of Field Robotics*, 23(1):3–20, 2006.

[9] Isaku Nagai and Yutaka Tanaka. *Mobile robot with floor tracking device for localization and*

control. *Journal of Robotics and Mechatronics*, 19(1):34–41, 2007.

[10] Masahiro Watanabe and Shree K. Nayar. *Telecentric optics for constant magnification imaging*. In *Columbia University, CUCS-026-95*, 1995.

[11] Genya Ishigami, Keiji Nagatani, and Kazuya Yoshida. *Slope traversal controls for planetary exploration rover on sandy terrain*. *Journal of Field Robotics (to be appeared)*, 2009

[12] R. Ranftl, V. Vineet, Q. Chen and V. Koltun, "Dense monocular depth estimation in complex dynamic scenes," in *Proceedings of the IEEE Conference on Computer Vision and Pattern Recognition*, 2016.

[13] S. Temizer, "Optical flow based local navigation," 2001.

[14] C. Kerl, J. Sturm and D. Cremers, "Dense visual SLAM for RGB-D cameras," in *Intelligent Robots and Systems (IROS), 2013 IEEE/RSJ International Conference on*, 2013.

[15] I. Dryanovski, C. Jaramillo and J. Xiao, "Incremental registration of RGB-D images," in *Robotics and Automation (ICRA), 2012 IEEE International Conference on*, 2012.

[16] Shashi Poddar, Rahul Kottath, Vinod Karar, *Evolution of Visual Odometry Techniques*, April 2018.

[17] Ming He, Chaozheng Zhu, *A review of monocular visual odometry*, June, 2019, DOI: 10.1007/s00371-019-01714-6